σ Bond Activation by Cooperative Interaction with ns^2 Atoms: Be + nH_2, $n = 1-3$

Stephanie B. Sharp and Gregory I. Gellene*

Department of Chemistry and Biochemistry, Texas Tech University, Lubbock, Texas 79409-1061

Received: June 27, 2000; In Final Form: September 8, 2000

Ab initio investigations at the MP2, CCSD(T), and MRCISD levels of theory with augmented triple-ζ basis sets have identified and characterized various stationary points on the Be/$(H_2)_n$, $n = 1-3$, hypersurfaces. The van der Waals complexes, Be$(H_2)_n$, are very weakly bound ($D_e = 0.08-0.32$ kcal/mol with respect to H_2 loss) with H_2/H_2 interactions playing an important role in determining equilibrium structures which can be understood in terms of the various relevant long-range potentials. The covalent molecule, BeH_2, is found to have a linear, centrosymmetric structure and to be strongly bound with respect to Be + H_2, in agreement with previous calculations. BeH_2 interacts weakly with additional H_2 molecules ($D_e < 0.75$ kcal/mol) which are positioned parallel to the near-linear BeH_2 moiety in the equilibrium structures of the $BeH_2(H_2)_{n-1}$ complexes. Of particular interest is the dramatic change in the nature of the transition state for BeH_2 production depending on the number of H_2 molecules present. For $n = 1$, the reaction proceeds stepwise: first breaking the H_2 bond and forming one BeH bond followed by forming the second BeH bond. This process has an activation energy of about 56 kcal/mol. For $n = 2$, the reaction proceeds via a pericyclic mechanism through a planar cyclic transition state where two H_2 bonds are broken while simultaneously two BeH bonds and one new H_2 bond are formed. The activation energy for this process decreases from the $n = 1$ value to about 38 kcal/mol. For $n = 3$, the reaction proceeds through a true insertion mechanism with the addition of the third H_2 molecule, decreasing the activation energy to about 33 kcal/mol. The results are discussed in comparison to the isoelectronic B^+/nH_2 systems where significant σ bond activation through a cooperative interaction mechanism has been identified.

Introduction

The formation of the covalently bound BeH_2 molecule by the reaction of Be with H_2 is a well-known difficult case for electronic structure theory. At the heart of the problem is the change of the principle $^1A_1$ electron configuration from $1a_1^2\ 2a_1^2\ 3a_1^2$ to $1a_1^2\ 2a_1^2\ 1b_2^2$ (in C_{2v} symmetry) as the system passes through the transition state region. Additional complications arise from the quasi-degeneracy of the Be 2s and 2p orbitals and the decreasing energy difference between the $1\sigma_g^2$ and $1\sigma_u^2$ electron configurations for H_2 as that internuclear separation increases. These features and the simplicity of possessing only four valence electrons has made the Be + H_2 symmetric insertion reaction a prototypic proving ground for a large variety of high level computational techniques.[1−10]

Recently, a new, qualitatively different motivation for studying BeH_2 has emerged. Kemper et al.,[11] using mass spectrometric techniques to study the interaction of B^+ (isoelectronic with Be) with H_2, discovered that the activation energy for forming BH_2^+ could be reduced from about 60 kcal/mol when only one H_2 molecule was present to approximately 2 kcal/mol when two additional H_2 molecules were present. Detailed understanding of the cooperative effect of the two additional H_2 molecules was provided by a theoretical analysis[12] of the reactions $B^+ + nH_2 \rightarrow BH_2^+ + (n-1)H_2$. The calculations revealed that the reaction mechanism and the nature of the transition state for BH_2^+ formation depended dramatically on the number of H_2 molecules present up to three. For $n = 1$, BH_2^+ is produced in a stepwise mechanism where first the H_2 bond is broken with one atom transferred to B^+ fully forming the first BH bond followed by formation of the other BH bond in a second step. For $n = 2$, BH_2^+ is produced in a concerted, one step process through a planar cyclic transition state with a pericyclic mechanism involving the simultaneous breaking of both H_2 bonds, while forming both BH bonds and a new H_2 bond. For $n = 3$, the reaction does proceed by direct insertion of B^+ into an H_2 bond but the insertion occurs very late in the reaction path after almost 75% of the reaction exothermicity has been released. A detailed analysis of the evolution of the molecular orbitals along the reaction paths for these three cases[12] revealed the origin of these dramatic mechanistic changes and their energetic consequences. To effectively weaken and ultimately break an H_2 bond, the node of an occupied molecular orbital must be "maneuvered" to bisect the H_2 molecule. With increasing number of H_2 molecules (up to three), the energy required to reach a transition state with the necessary orbital node position is increasingly offset by the formation of a corresponding number of favorable BH interactions.

Originally, with the phenomena observed and analyzed only for the $B^+ + nH_2$ systems, it was unclear how much of the activation energy lowering could be attributed to the node structure of the orbitals, how much could be attributed to the effects of the positive charge or how much could be attributed to the special ability of boron to participate in three center-two electron (3c−2e) bonds. Some evidence that 3c−2e bonding is important was inferred from the results of theoretical study of the isovalent systems,[13] $Al^+ + nH_2$, where similar reaction mechanisms were found only for the $n = 1$ and $n = 2$ cases. Additional support for the important role of 3c−2e bonding was provided by a theoretical study of the isoelectronic systems,[14] $Li^- + nH_2$, where a novel 3c−2e bonding scheme was identified in the transition state of the $n = 3$ case. However, detailed

10.1021/jp002313m CCC: $19.00
Published on Web 10/21/2000

comparisons with the corresponding $B^+ + nH_2$ systems were complicated by the competition between Li and H (becoming present as an H_2 molecule dissociates) for the negative charge which has no analogue in the cationic boron systems.

The present study of the $Be + nH_2$ reaction systems offers the possibility of gaining additional insight into the cooperative interaction mechanism. Because Be is isoelectronic with B^+, the molecular orbitals of $Be + nH_2$ are expected to correspond strongly with those of $B^+ + nH_2$, and being electrically neutral, the complications arising from charge competition are prevented. Furthermore, although 3c−2e bonding is more prevalent in boron chemistry, there is precedent for hydrogen bridge bonding in beryllium compounds. Several preparations have been reported[15−23] for BeH_2 which give a polymeric solid believed to contain BeH_2Be hydrogen bridge groups[21−23] which has been characterized by a stretching mode[24] centered near 1340 cm^{-1} but not, to date, by high quality X-ray diffraction.[23] However, crystal structures[25] have provided definitive evidence for BeH_2-Be hydrogen bridge bonding in alkylberyllium hydride derivatives.[24] Finally, the prototypic beryllium hydrogen bridge bonding molecule, $HBeH_2BeH$, has been identified in argon matrixes[26] as a product of laser evaporated beryllium reacting with hydrogen. Thus, to help assess the relative importance of charge and 3c−2e bonding in σ bond activation by cooperative interaction with an ns^2 electron configuration atom, a high level ab initio investigation of the reactions

$$Be(H_2)_n + H_2 \rightarrow BeH_2(H_2)_n \qquad n = 0-2 \qquad (1)$$

was performed. In reaction 1, $Be(H_2)_n$ denotes van der Waals complex and $BeH_2(H_2)_n$ denotes the covalently bound BeH_2 molecule interacting with additional H_2 molecules.

Motivated by structural, thermochemical, and polymerization questions and attracted by the low number of valence electrons, many theoretical investigations of BeH_2 (refs 27−42) and $(BeH_2)_x$ (refs 33−36, 38, 42) have been reported. The calculations indicate that BeH_2 is a linear, symmetric molecule with a BeH bond length of about 1.33 Å and dissociation energy of about 35−40 kcal/mol with respect to $Be + H_2$. Calculations on polymeric species, $(BeH_2)_x$, consistently find a hydrogen bridge bonding motif as the lowest energy structure. Matrix isolation infrared spectra[26] for BeH_2 and $(BeH_2)_2$ are constant with the theoretical predictions for the vibrational frequencies. To our knowledge, experimental evidence for the van der Waals complex, $Be(H_2)$, has not been reported. The interaction of Be with multiple H_2 molecules appears not to have been considered previously.

Methods

In general, triple-ζ valence Gaussian basis sets employing pure spherical harmonic functions were used. Valence and polarization functions were provided by the cc-pVTZ basis sets for hydrogen[43] and beryllium.[44] The hydrogen basis set was augmented by the diffuse functions recommended for use with the cc-pVTZ basis.[45] For beryllium, a set of diffuse functions for use with the cc-pVTZ basis set appears not to have been developed previously and exponents for an uncontracted (1s1p1d1f) set (s: 0.116; p: 0.018; d: 0.068; f: 0.142) were determined by optimizing the total energy of the excited $2s^12p^1$ ^1P atomic state at the complete active space (CAS) multiconfigurational self-consistent-field (MCSCF)[46,47] level followed by internally contracted configuration interaction in the single and double space (MRCISD).[48,49] In these MCSCF calculations, the 1s atomic orbital of beryllium was always doubly occupied and the two valence electrons were distributed among the four orbitals arising from the 2s and 2p atomic orbitals.

Stationary points on the $Be(H_2)_n$ and $BeH_2(H_2)_{n-1}$ hpersurfaces were generally located and characterized with second-order Møller−Plesset (MP2) perturbation theory applied to a Hartree−Fock (HF) wave function with frozen core electrons. Analytical first derivatives were used to optimize geometric structures to a residual root-mean-square force of less than 10^{-6} hartree/bohr and analytical second derivatives were used to characterize the stationary point as a local minimum (all real frequencies) or a transition state (one imaginary frequency). For each transition state identified for these systems, the reaction coordinate was determined by displacing the geometry slightly in the direction of the eigenvector associated with the imaginary frequency (both positive and negative) and following the potential energy gradient to a subsequent stationary point on the potential surface. In addition, at stationary points identified by the MP2 calculations, MRCISD and coupled cluster with single and double substitutions and a perturbative treatment of triple substitutions (CCSD(T))[50] calculations were performed. These additional single point calculations allow two issues to be addressed. First, CCSD(T) is a better method for electron correlation than MP2. And second, a comparison of the CCSD-(T) and MRCISD results gives insight into the validity of using single configuration approaches (i.e., MP2 and CCSD(T)).

An important exception to this general approach was followed for the characterization of the transition state region of the $n = 1$, Be/H_2 system. Because this region of that potential energy surface is necessarily multiconfigurational,[1−10] it could not be described well by MP2 calculations based on a single configuration HF wave function. Instead, this transition state was characterized by MRCISD. In the CAS-MCSCF portion of these calculations, the 1s orbital of Be was always doubly occupied and the four valence electrons were distributed among the six orbitals arising from the 2s and 2p atomic orbitals of beryllium and the 1s orbital of each hydrogen. Additionally, the $Be(H_2)$ and BeH_2 geometries were optimized at the CCSD(T) level. The MP2 and CCSD(T) calculations were performed with the GAUSSIAN 94 suite of programs[51] and the MRCISD calculations were performed with the MOLPRO[52] electronic structure package. All calculations were performed on a DEC alpha 3000/700 workstation.

Results

To simplify comparisons between the properties of various Be/nH_2 stationary points and the corresponding isoelectronic B^+/nH_2 stationary points,[12] only a subset of internal coordinates and harmonic frequencies will be reported here. A full description of the optimized geometries and harmonic frequencies will be provided as Supporting Information. The coordinates R, $r(H_2)$, and $\theta_{R,r(H_2)}$ will be used to denote the distance between Be and the midpoint of an H_2 molecule, the H_2 bond length, and the angle between R and $r(H_2)$, respectively. The coordinates r(BeH) and θ_{HBeH} will denote the BeH bond length and the HBeH bond angle in the BeH_2 moiety of a $BeH_2(H_2)_{n-1}$ complex or the transition state forming it. The angle formed by two different R coordinates will be denoted $\theta_{R,R'}$. The total energy of $Be(H_2)_n$ and $BeH_2(H_2)_{n-1}$ and harmonic zero point energies (ZPEs) are reported relative to the energies of the infinitely separated $Be + nH_2$ reactants. Unscaled MP2 harmonic frequencies are used in the calculation of ZPEs. Because MP2 and CCSD(T) are size extensive, the total energy of multiple H_2 molecules is simply the corresponding multiple of the single

TABLE 1: Calculated Geometry[a] and Relative Energy for Be(H_2) and BeH_2 Stationary Points

property	van der Waals complex	transition state	covalent molecule
point group	$C_{\infty v}$	C_s	$D_{\infty h}$
R (Å)/MP2	4.227		
R (Å)/CCSD(T)	4.563		
R (Å)/MRCISD		2.498	
$r(H_2)$ (Å)/MP_2	0.7377		
$r(H_2)$ (Å)/CCSD(T)	0.7433		
$r(H_2)$ (Å)/MRCISD		3.496	
r(BeH) (Å)/MP2			1.332
r(BeH) (Å)/MRCISD		1.350	
	Relative Energy[b]		
MP2	0.956		−40.70
CCSD(T)	−0.084		−36.56
MRCISD	−2.375	+58.83	−38.96
MRCISD+Q	0.591	+60.53	−35.33
	Relative ZPE[b]		
per-H	+0.22[c]	−3.49[d]	+1.79[c]
per-D	+0.15[c]	−2.37[d]	+1.26[c]

[a] With aug-cc-pVTZ basis set for H and the cc-pVTZ basis set augmented as described in the text for Be. [b] With respect to Be + H_2 (D_2) in kcal/mol. [c] At MP2 level of theory. [d] At MRCISD level of theory.

H_2 molecule energy. Unfortunately, MRCISD calculations do not enjoy this property. Consequently, MRCISD energies can be compared properly only when the calculations consider the same number of H_2 molecules (i.e., the supermolecule approach). Davidson[53] has proposed a correction (Q) to partially compensate for the size nonextensivity of MRCISD calculations and MRCISD+Q energies will also be reported as appropriate.

Variations in the H_2 bond length and harmonic stretching frequency are important indicators of 3c−2e bonding and the present results are compared with the previously reported[12] MP2/aug-cc-pVTZ values of 0.7374 Å and 4518 cm^{-1}, respectively, for isolated H_2.

Be and BeH. Calculations on Be and BeH were performed to evaluate the adequacy of the basis sets and methodologies. Excitation energies calculated for Be at the MRCISD level (with the experimental value[54] in parentheses) are $^3P \leftarrow {}^1S$ 22 048 cm^{-1} (21 980 cm^{-1}) and $^1P \leftarrow {}^1S$ 42 881 cm^{-1} (42 565 cm^{-1}), where a degeneracy weighted average experimental excitation energy of the ^3P_J states has been used. These calculated energies are within 1% of the experimental values. For BeH, r_e and ω_e calculated at the MP2 level (with the experimental values[55] in parentheses) are 1.3440 Å (1.3426 Å) and 2092.6 cm^{-1} (2060.8 cm^{-1}). These calculated values are within 1.5% of the experimental values. Thus, the present methodology was deemed sufficient to describe Be- -H interactions and the involvement of Be p orbitals required for covalent bonding.

Be(H_2) and BeH_2. Geometric and energetic parameters characterizing various stationary points on this hypersurface are summarized in Table 1 and illustrated in Figure 1. The van der Waals complex is calculated to be linear ($C_{\infty v}$) with R equal to 4.23 Å (MP2) and 4.56 Å (CCSD(T)). This seemingly large geometry discrepancy is put into perspective when it is recognized that a 0.3 Å displacement in R near the minimum energy structure results in an MP2 energy change of only about 0.01 kcal/mol. The H_2 moiety is little changed from its isolated characteristics with $r(H_2)$ increasing by 0.26 mÅ (MP2) or 5.7 mÅ (CCSD(T)), and $\omega(H_2)$ decreasing by only 9 cm^{-1} (MP2). Dissociation energies (D_e) showed considerable variability with the four methods investigated. MP2 and MRCISD+Q predict negative D_e values (i.e., the energy of the complex is greater than that of the Be + H_2) although the MP2 stationary point is a local minimum, MRCISD predicts a substantial D_e of 2.4 kcal/mol, and CCSD(T) predicts a modest D_e of 0.084 kcal/mol. Inclusion of MP2 harmonic ZPE predicts D_0 values which are decreased from D_e by 0.22 and 0.15 kcal/mol for the perhydrogenated and perdeuterated species, respectively.

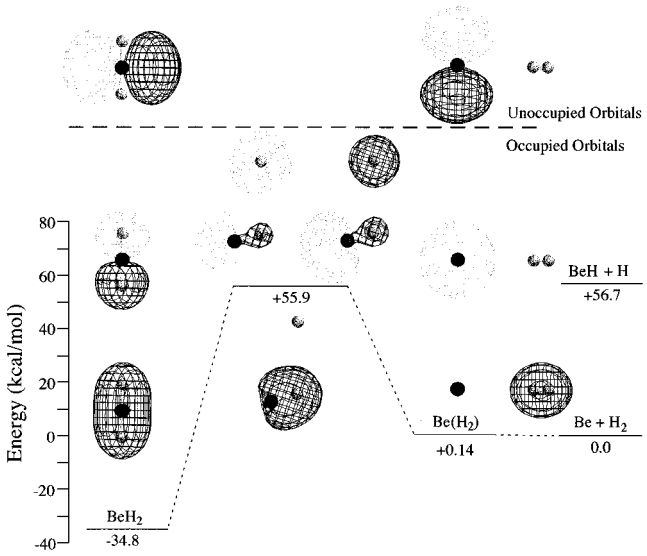

Figure 1. Relative energy of the stationary points on the minimum energy path for Be + $H_2 \rightarrow BeH_2$ calculated at the CCSD(T) level of theory with harmonic MP2 ZPE added for the perhydrogenated species The transition state energy and ZPE was calculated at the MRCISD level of theory. The orbitals pictured show the evolution of the two highest occupied and lowest unoccupied valence orbitals along the reaction path. The energy scale does not apply to the orbitals.

The covalent molecule is calculated to be linear and centrosymmetric ($D_{\infty h}$) with r(BH) equal to 1.33 Å (MP2) and 1.35 Å (CCSD(T)). The D_e values calculated by the four methods are in reasonable agreement with MP2 predicting a somewhat higher value of 40.7 kcal/mol and the CCSD(T), MRCISD, and MRCISD+Q values falling in the range 37.0 ± 2.0 kcal/mol. The MP2 harmonic frequencies for the perhydrogenated species are calculated to be 2056.5, 722.3, and 2265.6 cm^{-1} for the symmetric stretching, bending, and asymmetric stretching modes, respectively. These results indicate that D_0 is decreased from D_e by 1.79 and 1.26 kcal/mol for the perhydrogenated and perdeuterated species, respectively.

The transition state for this system is found to have a very asymmetric geometry with the short r(BH) equal to 1.353 Å and a long r(BH) equal to 4.10 Å. Although the H_2 molecule in this structure is essentially completely dissociated with $r(H_2)$ equal to 3.50 Å, θ_{HBeH} is only about 20°; a value far from 180° equilibrium value of the covalent molecule. The energy of this transition state is calculated to be 58.8 and 60.5 kcal/mol at the MRCISD and MRCISD+Q level of theory, respectively. Inclusion of MRCISD harmonic ZPE decreases the transition state energy by 3.49 and 2.37 kcal/mol for the perhydrogenated and perdeuterated species, respectively.

Be(H_2)$_2$ and BeH_2(H_2). Geometric and energetic parameters characterizing various stationary points on this hypersurface are summarized in Table 2 and illustrated in Figure 2. The van der Waals complex is calculated to have a planar C_s structure with MP2 R values of 4.32 and 4.18 Å which are very similar to that calculated for Be(H_2). Also similar to the $n = 1$ van der Waals complex, the H_2 molecules are nearly unchanged by the interaction with $r(H_2)$ increasing by less than 0.5 mÅ and $\omega(H_2)$ decreasing by less than 11 cm^{-1}. However, the orientation of

TABLE 2: Calculated Geometry[a] and Relative Energy for $Be(H_2)_2$ and $BeH_2(H_2)$ Stationary Points

property	van der Waals complex	transition state	covalent molecule
point group	C_s	C_{2v}	C_{2v}
R (Å)	4.3211 (∥)[b]	1.5663	2.8685
	4.1833 (⊥)[b]		
$r(H_2)$ (Å)	0.7379 (∥)[b]	0.9018	0.7391
	0.7377 (⊥)[b]		
r(BeH) (Å)		1.5027	1.3325
θ_{HBeH} (deg)		107.5	177.9
$\theta_{R,r(H_2)}$ (deg)	159.6 (∥)[b]	73.6	90.0
	123.3 (⊥)[b]		
$\theta_{R,R'}$ (deg)	46.5	74.0	
	Relative Energy[c]		
MP2	1.82	36.01	−40.20
CCSD(T)	−0.21	34.95	−37.15
MRCISD		31.75	−40.19
MRCISD+Q		36.11	−35.35
	Relative ZPE[c]		
per-H	0.67	3.31	2.84
per-D	0.47	2.33	2.01

[a] MP2 calculations with aug-cc-pVTZ basis set for H and cc-pVTZ basis set augmented as described in the text for Be. [b] (∥) and (⊥) refer to the H_2 for which $\theta_{R,r(H_2)}$ is more nearly 90° and 180°, respectively. [c] With respect to Be + H_2 (D_2) in kcal/mol.

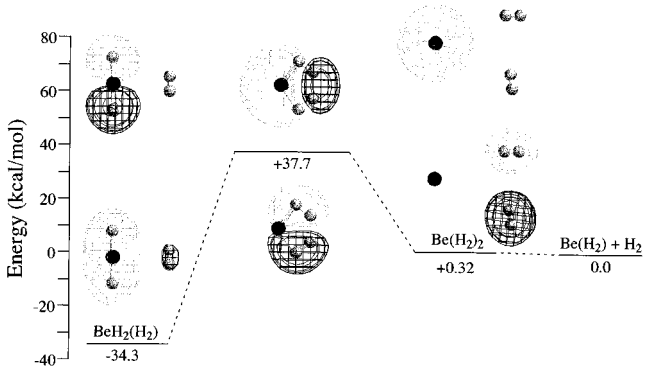

Figure 2. Relative energy of the stationary points on the minimum energy path for $Be(H_2) + H_2 \rightarrow BeH_2(H_2)$ calculated at the CCSD(T) level of theory with harmonic MP2 ZPE added for the perhydrogenated species. The orbitals pictured show the evolution of the two highest occupied and lowest unoccupied valence orbitals along the reaction path. The energy scale does not apply to the orbitals.

the H_2 molecules with respect to the Be atom in the $n = 2$ complex differ significantly from the linear configuration of the $n = 1$ complex with $\theta_{R,r(H_2)}$ values of 123° and 160°. Calculated D_e values are similar to the $n = 1$ results with CCSD(T) theory predicting the complex to be stable by about 0.21 kcal/mol. Inclusion of MP2 ZPE predicts that D_e is decreased by 0.67 and 0.47 kcal/mol for the perhydrogenated and perdeuterated species, respectively.

The structure of the covalently bound BeH_2 interacting with an additional H_2 molecule is calculated to be a planar, C_{2v} geometry. The geometric parameters of the BeH_2 (r(BH) = 1.3325 Å; $\theta_{HBH} = 178°$) and H_2 ($r(H_2) = 0.7391$ Å) moieties are nearly unchanged from their infinitely separated values. Similarly, the bending and stretching vibrations of BeH_2 in the complex are within 3 cm^{-1} of their isolated values and the H_2 stretch is decreased by only 30 cm^{-1}. Consistent with the weak interaction between BeH_2 and H_2, D_e values calculated by CCSD(T), MRCISD, and MRCISD+Q theory are increased by about 1 kcal/mol or less from the corresponding value calculated for BeH_2. Although the MP2 calculations converged to a local minimum energy structure, the energy is greater than that of $BeH_2 + H_2$. Inclusion of MP2 ZPE predicts that D_e is decreased by 2.84 and 2.01 kcal/mol for the perhydrogenated and the perdeuterated species, respectively.

TABLE 3: Calculated Geometry[a] and Relative Energy for $Be(H_2)_3$ and $BeH_2(H_2)_2$ Stationary Points

property	van der Waals complex	transition state	D_{3h} structure	covalent molecule
point group	C_3	C_{3v}	D_{3h}	C_{2v}
R (Å)	4.2462	1.8187	1.3124	2.8187
$r(H_2)$ (Å)	0.7379	0.7935	0.9129	0.7394
r(BeH) (Å)		1.7120	1.3895	1.3334
θ_{HBeH} (deg)		90.5	123.6	176.2
$\theta_{R,r(H2)}$ (deg)	69.2	68.3	90.0	90.0
$\theta_{R,R'}$ (deg)	49.4	72.6	120.0	71.7
	Relative Energy[b]			
MP2	2.60	28.13	4.31	−39.82
CCSD(T)	−0.53	25.97	5.61	−37.86
MRCISD	−3.76	23.62	3.88	−40.77
MRCISD+Q	0.12	27.31	5.70	−36.11
	Relative ZPE[b]			
per-H	1.19	8.14	9.67	4.10
per-D	0.84	5.75	6.83	2.90

[a] MP2 calculations with aug-cc-pVTZ basis set for H and cc-pVTZ basis set augmented as described in the text for Be. [b] With respect to Be + H_2 (D_2) in kcal/mol.

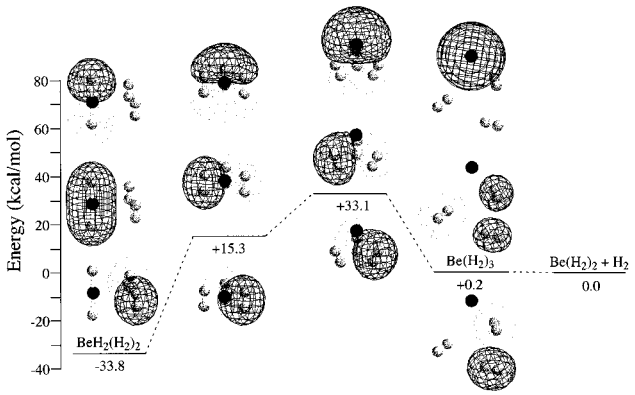

Figure 3. Relative energy of the stationary points on the minimum energy path for $Be(H_2)_2 + H_2 \rightarrow BeH_2(H_2)_2$ calculated at the CCSD-(T) level of theory with harmonic MP2 ZPE added for the perhydrogenated species. The orbitals pictured show the evolution of the two highest occupied and lowest unoccupied valence orbitals along the reaction path. The energy scale does not apply to the orbitals.

The transition state for this system was determined to be a five-membered ring having C_{2v} symmetry. In passing through this transition state from the van der Waals complex, the covalent molecule is formed through a pericyclic mechanism where simultaneously two H_2 bonds are broken, and two BeH bonds and one new H_2 bond are formed. At the transition state, r(BeH) is 0.17 Å longer than its equilibrium value in BeH_2 and $r(H_2)$ is about 0.16 Å longer than its equilibrium value in H_2. The energy of this transition state calculated by the four methods investigated covers the range of 34.3 ± 1.8 kcal/mol. Inclusion of MP2 ZPE predicts that the transition state energy is increased by 3.31 and 2.33 kcal/mol for the perhydrogenated and the perdeuterated species, respectively.

$Be(H_2)_3$ and $BeH_2(H_2)_2$. Geometric and energetic parameters characterizing various stationary points on this hypersurface are summarized in Table 3 and illustrated in Figure 3. The van der Waals complex is calculated to have a C_3 structure with $\theta_{R,r(H_2)} = 69.2°$ and MP2 R values of 4.25 Å, a value very similar to those calculated for $Be(H_2)$ and $Be(H_2)_2$. Again, the H_2 moiety is almost unchanged with $r(H_2)$ increased by only 5 mÅ and

$\omega(H_2)$ decreased by only 9 cm^{-1}. As with the other van der Waals clusters, MP2 and MRCISD+Q methods predict negative D_e values, MRCISD predicts a substantial D_e of 3.8 kcal/mol, and CCSD(T) predicts a modest D_e of 0.53 kcal/mol. Inclusion of MP2 ZPE predicts a D_0 which is decreased from D_e by 1.19 and 0.84 kcal/mol for the perhydrogenated and the perdeuterated species, respectively.

The structure of the covalently bound BeH_2 interacting with two H_2 molecules is calculated to have a C_{2v} geometry with the H_2 molecules parallel to the nearly linear ($\theta_{HBeH} = 176°$) BeH_2 moiety. As was the case with the $BeH_2(H_2)$ complex, the bond lengths and vibrational frequencies of the BeH_2 and H_2 subunits are almost unchanged from the corresponding infinitely separated values. D_e values calculated by MP2 and MRCISD+Q methods is less than that determined for $BeH_2(H_2)$ where as D_e values calculated by CCSD(T) and MRCISD methods is about 0.2−0.7 kcal/mol greater than that determined for $BeH_2(H_2)$. Inclusion of MP2 ZPE predicts a D_0 which is decreased from D_e by 4.10 and 2.90 kcal/mol for the perhydrogenated and the perdeuterated species, respectively.

The transition state for the $n = 3$ system has C_{3v} symmetry with R contracted to 1.82 Å, and the H_2 molecules elongated to $r(H_2) = 0.794$ Å. The value of r(BeH) is 1.71 Å and $\omega(H_2)$ has decreased by about 980 cm^{-1} from its infinitely separated value. The energy of this transition state calculated by the four methods investigated to fall in the range of 26.3 ± 1.9 kcal/mol. Inclusion of MP2 ZPE predicts that this transition state energy is increased by 8.14 and 5.75 kcal/mol for the perhydrogenated and the perdeuterated species, respectively. In passing through this transition state toward the covalent molecule, the C_3 symmetry axis is preserved along the minimum energy pathway leading to a highly symmetric D_{3h} structure. In this geometry, all six hydrogen atoms are equivalent with r(BeH) = 1.39 Å and $r(H_2) = 0.913$ Å. The energy of this structure is calculated by the four methods investigated to be 4.9 ± 1.0 kcal/mol. Although MP2 calculations characterize this stationary point as a local minimum, there is concern about the accuracy of this result. The MP2 transition state separating the D_{3h} structure from $BeH_2(H_2)_2$ is only very slightly distorted from the D_{3h} geometry and has an energy only 0.1 kcal/mol greater than the D_{3h} energy. Furthermore, the CCSD(T) energy of this near-D_{3h} transition state structure is lower than that of the D_{3h} structure. This uncertainty about the nature of the D_{3h} stationary point complicates estimating the associated ZPE. If it is treated as a local minimum then the relative ZPE is 9.67 and 6.83 kcal/mol for the perhydrogenated and perdeuterated species, respectively. However, if the structure is actually a transition state, the pair of e′ normal modes leading to $BeH_2(H_2)$ is expected to have with an imaginary frequency. Adjusting for the energy of this e′ mode pair predicts that, if the D_{3h} structure is a transition state, its ZPE is decreased by 2.23 and 1.58 kcal/mol for the perhydrogenated and perdeuterated species, respectively.

Discussion

Instructive trends in the results can be identified by grouping the systems as van der Waals complexes, covalent molecule, and the intervening transition states. It is also instructive to consider the relative energetics for stepwise addition of each H_2 molecule within these groups. Although this information is implicit in Tables 1−3, it is provided in Table 4 for convenience. Table 4 was constructed generally using CCSD(T) electronic energies and MP2 harmonic frequencies. The CCSD(T) energies are emphasized because only this methodology gave realistic interaction energies for the van der Waals clusters and because it facilitates comparisons with previous work on the isoelectronic B^+/nH_2 systems.[12] An important exception is the Be/H_2 transition state for which MRCISD energies and harmonic frequencies were used.

TABLE 4: Calculated Energy Changes[a] (kcal/mol) for the Indicated Reactions

reaction	electronic	per-H_2	per-D_2
van der Waals complex formation			
$Be + H_2 \rightarrow Be(H_2)$	−0.08	+0.14	+0.07
$Be(H_2) + H_2 \rightarrow Be(H_2)_2$	−0.13	+0.32	+0.19
$Be(H_2)_2 + H_2 \rightarrow Be(H_2)_3$	−0.32	+0.20	+0.05
Covalent Molecule Formation			
$Be + H_2 \rightarrow BeH + H$	+59.59	+56.68	+57.08
$Be + H_2 \rightarrow BeH_2$	−36.56	−34.77	−35.30
$BeH_2 + H_2 \rightarrow BeH_2(H_2)$	−0.58	+0.47	+0.17
$BeH_2(H_2) + H_2 \rightarrow BeH_2(H_2)_2$	−0.71	+0.55	+0.18
Transition State Formation			
$Be + H_2 \rightarrow (Be(H_2))^\dagger$	+59.39[b]	+55.90[b]	+57.02[b]
$Be(H_2) + H_2 \rightarrow (Be(H_2)_2)^\dagger$	+35.03	+37.67	+36.90
$Be(H_2)_2 + H_2 \rightarrow (Be(H_2)_3)^\dagger$	+26.10	+33.05	+31.00

[a] CCSD(T) electronic energy and MP2 ZPE with aug-cc-pVTZ basis set for H and cc-pVTZ basis set augmented as described in the text for Be. [b] MRCISD calculations.

van der Waals Complexes. The geometry of the van der Waals clusters can be understood in terms of the various long-range potentials (V_{LR}) involving the polarizability of Be (α_{Be}) and H_2 (α_{H_2}) and the permanent quadrupole moment of H_2 (Q_{H_2}). For $n = 1$ the leading term in V_{LR} is the dispersion term[56] proportional to $\alpha_{Be}\alpha_{H_2}/R^6$ (the leading induction term is proportional to $\alpha_{Be}Q_{H_2}/R^8$)[56] and, because the component of α_{H_2} parallel to the H_2 bond axis is about 40% larger than the perpendicular component,[57,58] the calculated linear $Be(H_2)$ geometry is expected. With the introduction of a second H_2 molecule in the $n = 2$ cluster, the leading term in V_{LR} becomes proportional to $Q_{H_2}^2/R$.[5] In an isolated $(H_2)_2$ cluster, the H_2 molecules adopt a T-shaped equilibrium geometry with a bond midpoint to bond midpoint separation ($R(H_2,H_2)$) calculated at the MP2/aug-cc-pVTZ level[59] to be 3.41 Å. The effect of this potential can be seen in the geometry of the $Be(H_2)_2$ cluster where the H_2 bond axes form angles of 91.6° and 7.9° with $R(H_2,H_2)$ which is equal to 3.36 Å. This pattern continues with the $Be(H_2)_3$ cluster where the H_2 bond axes form angles of 101.7° and 21.6° with $R(H_2,H_2)$ which equals 3.65 Å in this case. The formation of near T-shaped H_2/H_2 structures in preference to near linear Be/H_2 structure in the $n = 2$, 3 complexes indicates that these species are best thought of as $(H_2)_{2,3}$ clusters interacting with a Be atom. With regard to the calculated D_e, the CCSD(T) values are probably the most realistic considering that the D_e of Be_2 is about 2.5 kcal/mol,[60,61] α_{Be} is about 7 times[62] greater than α_{H_2}, and the Be/Be interaction is not entirely van der Waals.[63] However, the results cannot be considered definitive because questions about the effect of increased basis set size and increased levels of electron correlation remain. These issues were not addressed because the current emphasis was on the cooperative σ bond activation mechanism. Finally, we note that for such weakly bound clusters, a harmonic approximation for estimating ZPEs is clearly inappropriate.

Covalent Molecule. In agreement with previous theoretical studies,[27−42] BeH_2 is calculated to have a linear, centrosymmetric structure. However, the present best estimate for D_0 (34.8 kcal/mol) is somewhat lower than most previous theoretical estimates.[31,32,37,39] The discrepancy can be attributed to the higher correlation used in the present study because the MP2 D_e (−40.7 kcal/mol) agrees with previous similar calculations. Similarly,

MP2 harmonic frequencies agree with previous theoretical predictions[26,37] and matrix isolation experimental results.[26] The interaction of additional H_2 with BeH_2 appears not to have been considered previously. Although D_e is calculated to be about 8 times greater than that of Be/H_2, the value is nevertheless relatively small being less than 1 kcal/mol. The magnitude of D_e and the small effect that the $BeH_2/(H_2)_{1,2}$ interaction has on the geometric and vibrational characteristics of either BeH_2 or H_2 identifies the interaction as dominantly noncovalent. This result contrasts sharply with the isoelectronic $BH_2^+/(H_2)_{1,2}$ interactions[12] which were shown to be covalent involving 3c−2e even though $BeH_2(H_2)_{1,2}$ adopt geometries generally similar to $BH_2^+(H_2)_{1,2}$. The increased strength of the $BeH_2/(H_2)_{1,2}$ interaction relative to that in $Be/(H_2)_{1-3}$ is probably best attributed to a decreased size of the frontier orbital, which is induced by the sp orbital hybridization in the Be−H covalent bonds, and which allows R to decrease by about 1.4 Å. The effect can be seen by comparing the orbitals in Figures 1 and 2. A similar argument was invoked to explain an analogous effect observed for the $Al^+/(H_2)_{1-3}$ and $AlH_2^+/(H_2)_{1,2}$ systems.[13]

Transition State Formation. One of the most interesting results of this study is the variation in transition state structure and properties with the number of H_2 molecules present. For $n = 1$, the transition state is calculated to be about 56 kcal/mol which is only about 1 kcal/mol less than the energy of BeH + H. This result coupled with a structure where the short r(BeH) is only about 5 mÅ longer than the BeH equilibrium bond length, and an essentially fully dissociated H_2 bond ($r(H_2) = 3.5$ Å) identifies this mechanism as sequential bond formation. Although, an asymmetric transition state appears not to have been considered previously,[1−10] it is clearly the true transition state for this reaction because the energy is more than 40 kcal/mol less than the symmetric, concerted, insertion transition state.[1,4,6,10] Nevertheless, the orbital symmetry arguments predicting a multiconfigurational wave function in the transition state region remain valid. The two orbitals shown in the transition state region of Figure 1, differ by being bonding or antibonding with respect to H_2, which has little energetic consequences at $r(H_2) = 3.5$ Å and thus the orbitals are comparably occupied at the transition state. Furthermore, because each of these orbitals correlates with either the HOMO orbital of $Be(H_2)$ or BeH_2, they provide the required multiconfigurational "bridge" between the van der Waals complex and the covalent molecule. For $n = 2$, the mechanism for weakening and ultimately breaking an H_2 bond completely changes. Figure 2 shows that at the transition state, the node in the HOMO is "maneuvered" to bisect both H_2 bonds causing them to lengthen by about 0.16 Å. At the same time, however, two BeH bondlike distances, which are only about 0.15 Å longer than the equilibrium value in BeH_2, are established. Thus, the energy required to length the H_2 bond is partially compensated for by the energy gained in the BeH interactions. Although a similar statement could be made in the $n = 1$ case (one BeH interaction compensating for one lost H_2 interaction at the transition state), the second BeH interaction is much more energetic than the first. For example, the D_e of BeH is about 49.8 kcal/mol[64] whereas the D_e of BeH_2 with respect to BeH + H is about 96.2 kcal/mol. Thus, with two BeH interactions possible in the $n = 2$ case, a substantial reduction in the activation energy of about 24 kcal/mol relative to the $n = 1$ case is possible.

For $n = 3$, three H_2 molecules interact equivalently with Be in the transition state and Figure 3 shows that the node in the HOMO has begun to bisect all three H_2 bonds. However, the H_2 bond lengths are only elongated by about 0.06 Å and r(BeH) is almost 0.5 Å longer than the equilibrium value in BeH_2. Nevertheless, this structure can be identified with 3c−2e Be−H−H bonding because the H_2 stretching energy falls by almost 1000 cm^{-1} from the free H_2 value. This 3c−2e bonding in the transition state accounts for the 8.9 kcal/mol decrease in the electronic activation energy relative to the $n = 2$ case. The 3c−2e bonding is particular apparent in the D_{3h} intermediate structure where $r(H_2)$ has elongated to 0.91 Å and the six equivalent r(BeH) are only about 0.06 Å longer than the equilibrium value in BeH_2. Further, the H_2 stretching energy in the D_{3h} structure is approximately 2000 cm^{-1} lower than the free H_2 value. Of the three detailed reaction mechanisms considered, only this final one can be properly considered as an insertion mechanism.

Comparison with B^+/nH_2. As stated in the Introduction, the major motivation for investigating the Be/nH_2 systems was to compare possible σ bond activation with the previous results for the isoelectronic B^+/nH_2 systems.[12] There are, in fact, some striking similarities and some important differences. For the three cases investigated ($n = 1-3$) the transition state structures of the corresponding B^+/nH_2 and Be/nH_2 systems are very similar. In addition, the activation energies for the two $n = 1$ systems differ by less than 1 kcal/mol because the D_e for BeH (49.8 kcal/mol) and BH^+ (47.7 kcal/mol) are almost equal. However, the energetic similarity does not persist to the $n = 2$ systems. With the shift to the pericyclic mechanism, the activation energy decreases by only 24.4 kcal/mol for the Be/nH_2 systems which is less than half of the 51.3 kcal/mol decrease for the B^+/nH_2 systems. This large energetic difference cannot be attributed to detailed geometric differences in the transition state structures. The bond lengths of the "separating" H_2 molecules differ by less than 0.03 Å, the bond lengths of the "forming" H_2 differ by less than 0.04 Å, and r(BeH) and r(BH) are within 0.16 and 0.24 Å of their equilibrium values, respectively. Alternatively, it is tempting to attribute the energetic difference to the differing strengths of the second BeH ($BeH_2 \rightarrow BeH + H$, $D_e = 96.2$ kcal/mol) and BH ($BH_2^+ \rightarrow BH^+ + H$, $D_e = 122$ kcal/mol) bonds because the $n = 2$ transition states have two nearly fully formed BeH of BH bonds. While, no doubt, these bond energy considerations make some contribution to the $n = 2$ activation energy difference between the beryllium and boron systems, a comparison to the isovalent Al^+/nH_2 systems[13] shows that a bond energy explanation is not complete. The structure of the $n = 1$ and $n = 2$ transition states for Al^+/nH_2 are very similar to the corresponding Be/nH_2 and B^+/nH_2 systems. And, although each of the sequential AlH bond energies ($AlH^+ \rightarrow Al^+ + H$, $D_e = 21.2$ kcal/mol; $AlH_2^+ \rightarrow AlH^+ + H$, $D_e = 78.9$ kcal/mol) is substantially less than the corresponding BeH bond energy, the activation energy decrease between $n = 1$ and $n = 2$ in the Al^+/nH_2 system of 36.1 kcal/mol is 50% greater than that in the Be/nH_2 system. Thus, the positive charge appears to play a more significant role than the individual bond energies in determining the energetic benefit of shifting the mechanism from sequential bond formation ($n = 1$) to concerted bond formation ($n = 2$).

Curiously, an energetic similarity emerges again for the $n = 3$ system where the activation energy decrease is 8.9 and 8.5 kcal/mol for the Be/nH_2 and B^+/nH_2 systems, respectively. The best explanation for this similarity seems to be the comparable ability of beryllium and boron to participate in 3c−2e, hydrogen bridge bonds. For example, the dimerization energy of BeH_2 and BH_3, each involving the formation of two 3c−2e, hydrogen bridge bonds, are 33.3 and 41.0 kcal/mol,[38] respectively. This hydrogen bridge bonding explanation is supported by the

absence of the effect in the $Al^+/3H_2$ system (the reaction has the $n = 2$ pericyclic transition state with a spectator H_2) where 3c−2e bonding is not usually expected. The hydrogen bridge bonding explanation also explains why the cooperative effect does not extend beyond the involvement of three σ bonds (i.e., $n = 3$). With the participation in three 3c−2e bonds and the two electrons nominally in the 2s orbital, B^+ or Be formally obtains a full octet of valence electrons.

Summarizing, the special ability of B^+ to promote σ bond activation through cooperative interaction involving up to three σ bonds appears to depend on a fairly unique combination of characteristics. Focusing on the cooperative effect (i.e., considering the sequential activation energy lowering), the following trend emerges. When two σ bonds in the form of H_2 are present, the stronger σ bonds that B^+ can form gives it a 15.2 kcal/mol advantage over Al^+, and the positive charge gives B^+ a 26.9 kcal/mol advantage over Be. Then, when a third H_2 σ bond is present, the ability to participate in 3c−2e hydrogen bridge bonding gives B^+ an 8.5 kcal/mol advantage over Al^+ and keeps it comparable to Be which also forms 3c−2e hydrogen bridge bonds.

Acknowledgment. We gratefully acknowledge the support of the Robert A. Welch Foundation and the Petroleum Research Fund, administered by the American Chemical Society, under Grant No. 33631-AC6, for partial support of this work.

Supporting Information Available: Tables giving the geometries and harmonic frequencies characterizing the various $Be(H_2)_n$ and $BeH_2(H_2)_{n-1}$ stationary points are available free of charge via the Internet at http://pubs.acs.org.

References and Notes

(1) Purvis, G. D., III; Shepard, R.; Brown, F. B.; Bartlett, R. J. *Int. J. Quantum Chem.* **1983**, *23*, 835.
(2) O'Neal, D.; Taylor, H.; Simons, J. *J. Phys. Chem.* **1983**, *88*, 1510.
(3) Laidig, W. D.; Bartlett, R. J. *Chem. Phys. Lett.* **1984**, *104*, 424.
(4) Page, M.; Saxe, P.; Adams, G. F.; Lengsfield, B. H., III. *J. Chem. Phys.* **1984**, *81*, 434.
(5) Zarrabian, S.; Laidig, W. D.; Bartlett, R. J. *Phys. Rev. A* **1990**, *41*, 4711.
(6) Valdemoro, C.; Bochicchio, R.; de Lara, M. P.; Tel, L. M. *J. Mol. Struct.* **1995**, *341*, 33.
(7) Smeyers, Y.; González-Guerra, A.; Martín-González, J.; Fernández-Serra, P. *Int. J. Quantum Chem.* **1996**, *60*, 493.
(8) Füsti-Molnár, L.; Szalay, P. G. *J. Phys. Chem.* **1996**, *100*, 6288.
(9) Chaudhuri, R. K.; Finley, J. P.; Freed, K. F. *J. Chem. Phys.* **1997**, *106*, 4067.
(10) Khait, Y. G.; Hoffmann, M. R. *J. Chem. Phys.* **1998**, *108*, 8317.
(11) Kemper, P. R.; Bushnell, J. E.; Weis, P.; Bowers, M. T. *J. Am. Chem. Soc.* **1998**, *120*, 7577.
(12) Sharp, S. B.; Gellene, G. I. *J. Am. Chem. Soc.* **1998**, *120*, 7585.
(13) Sharp, S. B.; Lemoine, B.; Gellene, G. I. *J. Phys. Chem. B* **1999**, *103*, 8039.
(14) Sharp, S. B.; Gellene, G. I. *J. Chem. Phys.*, in press.
(15) Pietsch, E. *Z. Elektrochem.* **1933**, *39*, 577.
(16) Wiberg, E.; Bauer, R. *Z. Naturforsch.* **1951**, *6b*, 171.
(17) Barbaras, G. D.; Dillard, C.; Finholt, A. E.; Wartik, T.; Wilzbach, K. E.; Schlesinger, H. I. *J. Am. Chem. Soc.* **1951**, *73*, 4585.
(18) Wiberg, E. *Angew. Chem.* **1953**, *65*, 16.
(19) Cotes, G. E.; Glockling, F. *J. Chem. Soc.* **1954**, 2526.
(20) Head, E. L.; Holly, C. E., Jr.; Rabideau, S. W. *J. Am. Chem. Soc.* **1957**, *79*, 3687.
(21) Mounier, J. *C. R. Acad. Sci. Paris Ser. C* **1967**, *265*, 1261.
(22) Baker, R. W.; Brendel, G. L.; Lowrance, B. R.; Mangham, J. R.; Marlett, E. M.; Shepherd, L. H., Jr. *J. Organomet. Chem.* **1978**, *159*, 123.
(23) Brendel, G. J.; Marlett, E. M.; Niebylski, L. M. *Inorg. Chem.* **1978**, *17*, 3589.
(24) Bell, N. A.; Coates, G. E. *J. Chem. Soc.* **1965**, 692.
(25) Adamson, G. W.; Shearer, H. M. M. *Chem. Commun.* **1965**, *11*, 240.
(26) Tague, T. J., Jr.; Andrews, L. *J. Am. Chem. Soc.* **1993**, *115*, 12111.
(27) Lao, R. C. C.; Riter, J. R., Jr. *J. Phys. Chem.* **1967**, *71*, 2737; **1967**, *71*, 3111.
(28) Hayes, E. F.; Pfeiffer, G. V. *J. Chem. Phys.* **1967**, *47*, 5168.
(29) Wu, A. A.; Ellison, F. O. *J. Chem. Phys.* **1968**, *48*, 727.
(30) Frost, A. A. *J. Phys. Chem.* **1968**, *72*, 1289.
(31) Ahlrichs, R.; Kutzelnigg, W. *Theor. Chim. Acta* **1968**, *10*, 377.
(32) Kaufman, J. J.; Sachs, L. M.; Geller, M. *J. Chem. Phys.* **1968**, *49*, 4369.
(33) Ahlrichs, R. *Theor. Chim. Acta* **1970**, *17*, 348.
(34) Dill, J. D.; Schleyer, P. v. R.; Binkley, J. S.; Pople, J. A. *J. Am. Chem. Soc.* **1977**, *99*, 6159.
(35) Marynick, D. S. *J. Am. Chem. Soc.* **1981**, *103*, 1328.
(36) Cimiraglia, R.; Persico, M.; Tomasi, J.; Charkin, O. P. *J. Comput. Chem.* **1984**, *5*, 263.
(37) Pople, J. A.; Luke, B. T.; Frisch, M. J.; Binkley, J. S. *J. Phys. Chem.* **1985**, *89*, 2198.
(38) DeFrees, D. J.; Raghavachari, K.; Schlegel, H. B.; Pople, J. A.; Schleyer, P. v. R. *J. Phys. Chem.* **1987**, *91*, 1857.
(39) Sana, M.; Leroy, G. *Theor. Chim. Acta* **1990**, *77*, 383.
(40) Sana, M.; Leroy, G.; Wilante, C. *Organometallics* **1991**, *10*, 264.
(41) Sana, M.; Leroy, G. *J. Mol. Struct. (THEOCHEM)* **1991**, *226*, 307.
(42) Bruna, P. J.; Di Labio, G. A.; Wright, J. S. *J. Phys. Chem.* **1992**, *96*, 6269.
(43) Dunning, T. H., Jr. *J. Chem. Phys.* **1989**, *90*, 1007.
(44) Basis set was obtained from the Extensible Computational Chemistry Environment Basis Set Database, Version 1.0, as developed and distributed by the Molecular Science Computing Facility, Environmental and Molecular Sciences Laboratory which is part of the Pacific Northwest Laboratory, P.O. Box 999, Richland, WA 99352, and funded by the U.S. Department of Energy. The Pacific Northwest Laboratory is a multiprogram laboratory operated by Battelle Marorial Institute for the U.S. Department of Energy under contract DE-AC06−76RLO 1830. Contact David Feller or Karen Schuchardt for further information. World Wide Web address: http://www.emsl.pnl.gov: 2080/forms/basisform.html.
(45) Kendal, R. A.; Dunning, T. H., Jr.; Harrison, R. J. *J. Chem. Phys.* **1992**, *96*, 6796.
(46) Werner, H.-J.; Knowles, P. J. *J. Chem. Phys.* **1985**, *82*, 5053.
(47) Knowles, P. J.; Werner, H.-J. *Chem. Phys. Lett.* **1985**, *115*, 259.
(48) Werner, H.-J.; Reinsch, E. A. *J. Chem. Phys.* **1988**, *89*, 5803.
(49) Knowles, P. J.; Werner, H.-J. *Chem. Phys. Lett.* **1988**, *145*, 514.
(50) Raghavachari, K.; Trucks, G. W.; Pople, J. A.; Head-Gordon, M. *Chem. Phys. Lett.* **1989**, *157*, 479.
(51) Frisch, M. J.; Trucks, G. W.; Schlegal, H. B.; Gill, P. M. W.; Johnson, B. G.; Robb, M. A.; Cheeseman, J. R.; Keith, T.; Petersson, G. A.; Montgomery, J. A.; Raghavachari, K.; Al-Laham, M. A.; Zakrzewski, V. G.; Ortiz, J. V.; Foresman, J. B.; Peng, C. Y.; Ayala, P. Y.; Chen, W.; Wong, M. W.; Andres, J. L.; Replogle, E. S.; Gomperts, R.; Martin, R. L.; Fox, D. J.; Binkley, J. S.; Defrees, D. J.; Baker, J.; Stewart, J. P.; Head-Gordon, M.; Gonzalez, C.; Pople, J. A. *Gaussian 94*, Revision B.3; Gaussian, Inc.: Pittsburgh, PA, 1995.
(52) MOLPRO is a package of ab initio programs written by H.-J. Werner and P. J. Knowles with contributions from: Almlöf, J.; Amos, R. D.; Deegan, M. J. O.; Elbert, S. T.; Hampel, C.; Meyer, W.; Peterson, K.; Pitzer, R.; Stone, A. J.; Taylor, P. R.; Lindh, R.
(53) Langhoff, S. R.; Davidson, E. R. *Int. J. Quantum Chem.* **1974**, *8*, 61.
(54) Moore, C. E. *Atomic Energy Levels as Derived from the Analysis of Optical Spectra*; U. S. Department of Commerce, National Bureau of Standards: Washington, DC, 1949; Vol. 1.
(55) Colin, R.; De Greef, D. *Can. J. Phys.* **1975**, *53*, 2142.
(56) Buckingham, A. D. *Adv. Chem. Phys.* **1967**, *12*, 107.
(57) Buckingham, A. D. *Proc. R. Soc. London A* **1966**, *295*, 334.
(58) Macadam, H. R. *Phys. Rev. A* **1977**, *6*, 898.
(59) Chang, D. T. Masters Thesis, Texas Tech University, 1998.
(60) Bondybey, V. E. *Chem. Phys. Lett.* **1984**, *109*, 436.
(61) Füsti-Molnár, L.; Szalay, P. G. *Chem. Phys. Lett.* **1996**, *258*, 400.
(62) Tunega, D.; Noga, J.; Klopper, W. *Chem. Phys. Lett.* **1997**, *269*, 435.
(63) Blomberg, M. R. A.; Siegbahn, P. E. M.; Roos, B. O. *Int. J. Quantum. Chem.* **1980**, *S14*, 229.
(64) Huber, K. P.; Herzberg, G. *Constants of Diatomic Molecules*; Van Nostrand Reinhold: New York, 1979.